Geological Survey of Canada

CURRENT RESEARCH
2006-C2

Characterization of hydrothermal alterations at the Red Lake mine, northwestern Ontario

A.-M. Cadieux, B. Dubé, K. Williamson, M. Malo, and T. Twomey

2006

Natural Resources Canada Ressources naturelles Canada

Canada

CURRENT RESEARCH

ISSN 1701-4387
Catalogue No. M44-2006/C2E-PDF
ISBN 0-662-43479-X

A copy of this publication is also available for reference by depository libraries across Canada through access to the Depository Services Program's Web site at http://dsp-psd.pwgsc.gc.ca

A free digital download of this publication is available from GeoPub: http://geopub.nrcan.gc.ca/index_e.php

Toll-free (Canada and U.S.A.): 1-888-252-4301

Critical reviewer
S. Castonguay

Authors' addresses

A.-M. Cadieux
INRS-Eau, Terre et Environnement
490 rue de la Couronne
Québec (Quebec) G1K 9A9

B. Dubé (***bdube@nrcan.gc.ca***)
Geological Survey of
Canada – Quebec
490 rue de la Couronne
Québec, Quebec G1K 9A9

K. Williamson
(***kenneth.williamson@goldcorp.com***)
Goldcorp Inc.
Red Lake Mine
Balmertown, Ontario P0V 1C0

M. Malo
(***Michel_Malo@inrs-ete.uquebec.ca***)
INRS-Eau, Terre et Environnement
490 rue de la Couronne
Québec (Quebec) G1K 9A9

T. Twomey
(***tim.twomey@goldcorp.com***)
Goldcorp Inc.,
Red Lake Mine
Balmertown, Ontario P0V 1C0

Publication approved by GSC Quebec

Original manuscript submitted: 2006-01-31
Final version approved for publication: 2006-02-02

Correction date:

Characterization of hydrothermal alterations at the Red Lake mine, northwestern Ontario

A.-M. Cadieux, B. Dubé, K. Williamson, M. Malo, and T. Twomey

Cadieux, A.-M., Dubé, B., Williamson, K., Malo, M., and Twomey, T., 2006: Characterization of hydrothermal alterations at the Red Lake mine, northwestern Ontario; Geological Survey of Canada, Current Research 2006-C2, 14 p.

Abstract: The aim of this study is to characterize the hydrothermal alteration of the High Grade zone at the Red Lake mine, with a focus on the altered basalts as they constitute the main host to the ore. These basalts were affected by 1) bleaching (aluminous alteration), 2) garnet-magnetite alteration, 3) emplacement of carbonate-magnetite breccias, 4) biotite-carbonate alteration, and 5) arsenopyrite-rich replacement. The mineralogical assemblages described in the current study confirm that the sampled rocks are transitional between greenschist- and amphibolite-grade conditions. The majority of the minerals in these assemblages were formed during deformation. The biotite-carbonate alteration and the arsenopyrite-rich replacement zones are clearly associated with the gold mineralization, and the biotite they contain has the characteristic composition of magnesian biotite. All alteration types show a lower Na_2O content than the least altered basalts. The biotite-carbonate alteration and the arsenopyrite-rich replacement zones, from which most of the mineralized samples were collected, show net mass gain due to a K_2O, S, CO_2 and SiO_2 increase compared to the basalt protolith.

Résumé : Cette étude vise à caractériser l'altération hydrothermale de la zone High Grade à la mine Red Lake, notamment des basaltes altérés puisqu'ils constituent les principales roches encaissantes du minerai. Ces basaltes ont subi (1) un blanchiment (altération alumineuse), (2) une altération en grenat-magnétite, (3) la formation de brèches à carbonates-magnétite, (4) une altération en biotite-carbonates et (5) un remplacement par un matériau riche en arsénopyrite. Les assemblages minéralogiques décrits dans cette étude confirment que les roches échantillonnées correspondent à un stade de transition entre le métamorphisme au faciès des schistes verts et le métamorphisme au faciès des amphibolites. La majorité des minéraux de ces assemblages se sont formés pendant la déformation. Les zones d'altération en biotite-carbonates et les zones de remplacement riches en arsénopyrite sont clairement associées à la minéralisation aurifère, et la biotite qu'elles renferment a une composition caractéristique de la biotite magnésienne. Tous les types d'altérations révèlent une teneur en Na_2O inférieure à celle des basaltes les moins altérés. Les zones d'altération en carbonates-biotite et les zones de remplacement riches en arsénopyrite, d'où proviennent la plupart des échantillons minéralisés, montrent un accroissement net de masse attribuable à des concentrations accrues de K_2O, de S, de CO_2 et de SiO_2, comparativement à celles du protolithe de basalte.

INTRODUCTION

The Red Lake gold district in northwestern Ontario is the second largest gold district in Canada with almost 1000 tons of Au (total includes Au both already produced and still remaining) (Fig. 1). Most of these tons are hosted within the giant Campbell-Red Lake deposit (>840 tons Au; Dubé et al., 2004; Gosselin and Dubé, 2005). This district hosts the number one Canadian gold producer, the Goldcorp Inc. Red Lake mine, including the High Grade zone (Fig. 1). The district is the focus of intense exploration, largely due to the discovery of the High Grade zone. Hydrothermal alteration is one key parameter to help finding extensions to these zones or discover new deposits.

In their study of the Red Lake greenstone belt, Andrews et al. (1986) reported intense alteration associated with gold mineralization spatially and temporally related to the contact-metamorphic aureoles around the adjacent batholiths. They described mafic volcanic rocks altered to quartz-ferroan dolomite-sericite-chlorite-calcite assemblages in greenschist-facies environments, and to quartz-biotite-muscovite-garnet-andalusite-staurolite-cordierite-chloritoid assemblages in amphibolite-facies environments. Damer (1997) separated the alteration assemblages at the Red Lake mine into three zones: 1) a distal zone with chlorite-plagioclase-garnet-andalusite-quartz-staurolite-chloritoid-biotite-ilmenite± cummingtonite; 2) an intermediate zone with hornblende-biotite-chlorite-plagioclase-quartz-ankerite-magnetite± anthophyllite; and 3) a proximal zone with biotite-ankerite-quartz-muscovite-plagioclase-magnetite±chlorite. Penczak and Mason (1999) subdivided the sequence of hydrothermal alteration at the Campbell mine into three phases: 1) an early alteration phase subdivided into a) carbonatization and pervasive biotite (potassic) alteration and b) early silicification and aluminosilicate-bearing alteration; 2) a main-stage vein phase of barren colloform-crustiform carbonate (dolomite to ankerite) and quartz veins, cockade breccias, and sheeted to stockwork veinlet zones with chloritic alteration; and 3) a mineralization phase with a quartz-sericite±cordierite

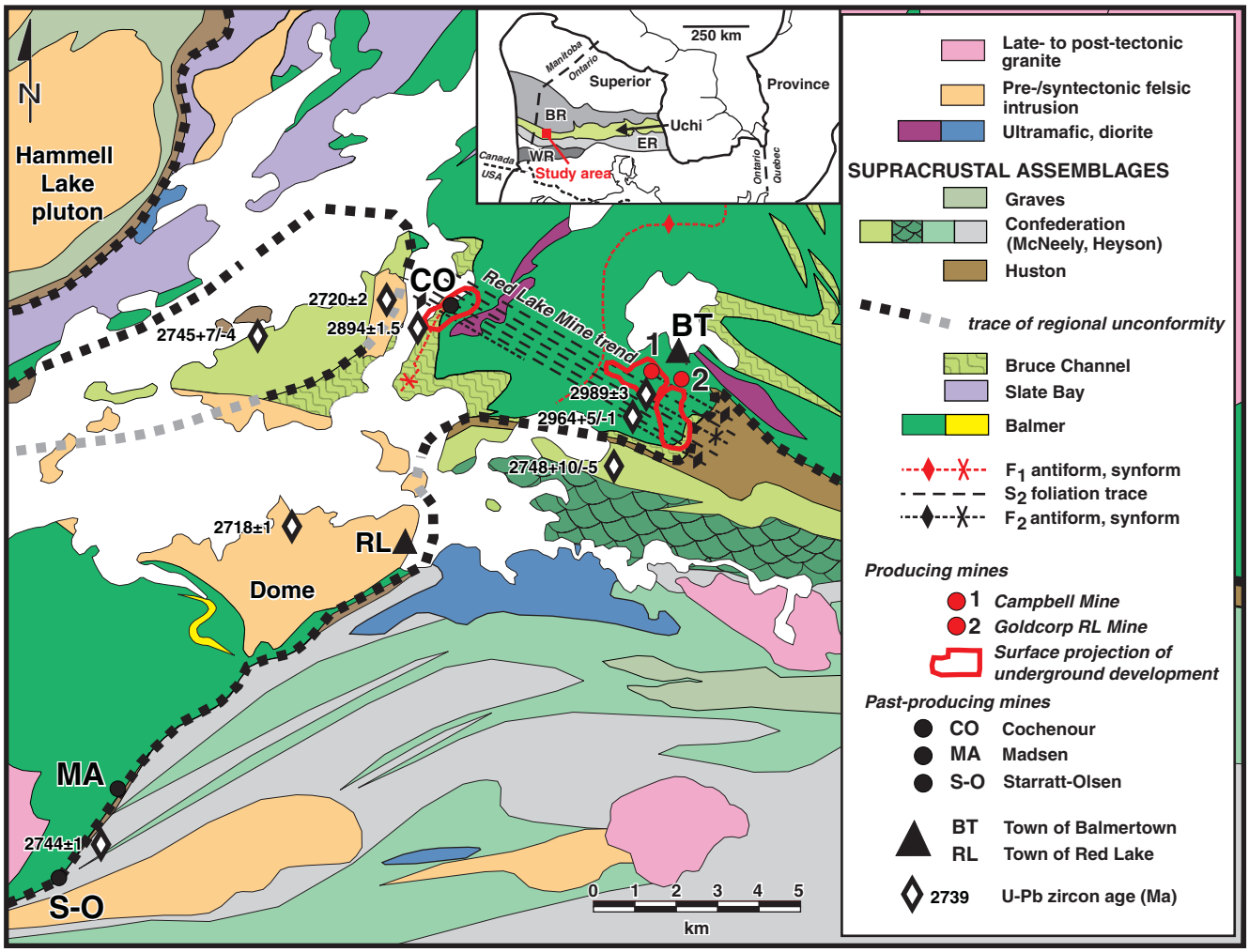

Figure 1. Geology of Red Lake mine trend area (*from* Dubé et al., 2003; *modified from* Sanborn-Barrie et al., 2001, and Goldcorp geological data).

alteration and a later episode of veinlet-controlled biotite±tourmaline alteration. Tarnocai (2000) presented almost the same sequence of events for the Campbell mine with four episodes of fracturing associated with hydrothermal alteration: 1) an aluminous alteration, 2) an iron carbonate pervasive alteration, 3) a first episode of gold mineralization, and 4) a second episode of gold mineralization controlled by pre-existing quartz-carbonate veins.

The purpose of the current study is to characterize the different alteration types mapped in the High Grade zone as well as the16th level of the Red Lake mine (Dubé et al., 2001, 2002, 2003). The study is based on 47 altered and five relatively fresh samples from the Balmer basalt, which constitutes the main host to the ore. A few samples of basaltic and peridotitic komatiites, and of the "pinky" granodiorite and feldspar porphyry dykes have also been examined.

REGIONAL AND LOCAL GEOLOGICAL SETTING

A brief summary of the geological setting of the Campbell-Red Lake deposit is presented below. Readers should refer to the following papers for more details: MacGeehan and Hodgson (1982), Andrews et al. (1986), Rogers (1992), Penczak and Mason (1997, 1999), Zhang et al. (1997), Tarnocai (2000), Sanborn-Barrie et al. (2001, 2004), Twomey and McGibbon (2001), and Dubé et al. (2001, 2002, 2003, 2004).

The Campbell-Red Lake gold deposit is hosted mainly by tholeiitic basalt and locally by komatiitic basalt of the Mesoarchean Balmer assemblage (Penczak and Mason, 1997) (Fig. 1). The mine sequence is completed by peridotitic komatiite, rhyolite and associated mafic intrusions of the Balmer assemblage (ca. 2.99–2.96 Ga), and felsic pyroclastic rocks with clastic and chemical sedimentary rocks of the Bruce Channel assemblage (ca. 2.984 Ga; Fig. 1; Penczak and Mason, 1997; Dubé et al., 2001). Based on relative chronology and U-Pb dating, the rocks of the mine area were affected by several generations of structures (*see* details in Dubé et al., 2002, 2004).

A recent assessment of metamorphic assemblages across the Red Lake greenstone belt by Thompson (2003) supports Christie's (1986) and Tarnocai's (2000) work, placing the Campbell-Red Lake deposit on the low-grade side of the lower boundary of the transition zone between greenschist and amphibolite facies, and less than 200 m from the biotite isograd marking the lower/upper greenschist-zone boundary.

The Campbell-Red Lake deposit is characterized by numerous barren to low-grade banded colloform-crustiform carbonate±quartz veins and cockade breccias (MacGeehan and Hodgson, 1982; Penczak and Mason, 1997; Tarnocai, 2000; Dubé et al., 2001, 2004). In addition, five different styles of gold mineralization are present: 1) sulphide-rich veins and replacement-style ore; 2) carbonate±quartz veins; 3) magnetite-rich ore; 4) high-grade arsenopyrite-rich silicification (replacement of carbonate±quartz veins/breccias and Balmer basalt) that typify the High Grade zone, (5) visible gold coating and filling late fractures (Penczak and Mason, 1997, 1999; Dubé et al., 2004). The High Grade zone contains great examples of styles 3, 4 and 5.

ALTERATION

Hydrothermal alteration in the Red Lake belt is distributed in large-scale and zoned alteration envelopes around gold deposits (Parker, 2000). The distal zone consists of belt-scale, moderate to intense calcite carbonatization, chloritization, and weak potassic alteration. Proximal zones, which vary in size from hundreds of metres to centimetres in width, are characterized by intense ferroan-dolomite and potassic alteration (Parker, 2000).

The Balmer basalt hosts most of the mineralization and is characterized by at least five hydrothermal-mineralogical assemblages at the Red Lake mine: 1) aluminous alteration (bleaching), 2) garnet-magnetite alteration, 3) carbonate-magnetite breccias, 4) biotite-carbonate alteration, and 5) arsenopyrite-rich replacement. The mineralogy of all samples was described in detail, except for that of the relatively fresh basalt, whose data come from Tomlinson (1998), Skulski (pers. comm., 2004) and Parker (2002). A compilation of mineral assemblages observed in the different alteration types is presented in Table 1. Electronic microprobe and geochemical analyses were also used to define the mineralogy and the alteration signature of each alteration type (Table 2).

MINERALOGY AND GEOCHEMISTRY

'Fresh' Balmer basalt

The mafic volcanic rocks of the Balmer assemblage are the most common host rock of the deposit. They are black, massive, very fine grained, pillowed, and locally variolitic basalts. The pillow margins are commonly filled with carbonate material and smaller amount of dark chlorite. Varioles are usually subrounded, filled with carbonate, and show a 1:1 to 4:1 shape ratio. The basalt hosts carbonate±quartz veins and veinlets that are very often subparallel or oblique to the main east-southeast-trending fabric (Dubé et al., 2001, 2002).

It should be specified that unaltered basalts are rare in the deposit due to the large size of the alteration system. In the current study, five analyses of relatively unaltered Balmer basalt from eastern Red Lake were used. These analyses were compiled by Skulski (pers. comm., 2004) from a major data set containing data from Tomlinson (1998), Parker (2002), and Skulski (unpub. data); and are characterized by less than

Table 1. Compilation of the mineral assemblages observed in the different alteration types.

Alteration type	PG		SR-PN	AM			Bi		MU	FC	Ch			CB				TC	QZ	AD	SU	CR	GT	EP	MG	IM	RU	PY	AsPY	PO	PD	CP	Gersd.	Ullm.
	AA	AN		Tsch.	HB	CG-AT	PH	Bi			Rip.	Penn.	Diab.	CC	Fe-DM	AK	MN																	
Bleached basalt (aluminous)		x	x					x			x	x							x	x	x	(x)	(x)	(x)	(x)	x	(x)	x		x	x	(x)	x	x
CB-MG breccias	x				x	x		x			x				x	x			x				x		x				(x)	x	x	(x)		
Bi-CB alteration in basalt	x				(x)	(x)		x	x					x	x	x			x						x		x	x	x	x	x	(x)		
GT-MG alteration in basalt	x		x	x		x		x			x		x		x	x			x	x	x	(x)	x	x	x	(x)		x	x	x	x	x		
AsPY replacement zones	x		x				x		x	x				x		x			x						(x)	(x)		x	x	x	(x)	(x)	(x)	
Basaltic komatiite Bi-CB		x						x	x	x	x				x	x			x						x			x	x	x	x			
Peridotitic komatiite CB	x											x					x	x							x			x						
"pinky" granodiorite dyke	x		x					x	x		x			x											x	x		x		x	x			

AA: anorthite; AD: andalusite; AK: ankerite; AM: amphibole; AN: andesine; AsPY: arsenopyrite; Bi: biotite; CB: carbonate; CC: calcite; CG-AT: cummingtonite-anthophyllite; Ch: chlorite; CP: chalcopyrite; CR: chloritoid; Diab.: diabantite; EP: epidote; FC: fuchsite; Fe-DM: Fe-dolomite; Gersd.: gersdorffite; GT: garnet; HB: hornblende; IM: ilmenite; MG: magnetite; MN: magnesite; MU: muscovite; PD: pentlandite; PG: plagioclase; PH: phlogopite; PO: pyrrhotite; PY: pyrite; Penn.: penninite; QZ: quartz; Rip.: ripidolite; RU: rutile; SR-PN: sericite-prehnite; SU: staurolite; TC: talc; Tsch.: tschermakite; Ullm.: ullmannite; (x) locally present and/or present as traces

Table 2. Geochemical analyses of samples from the Red Lake mine.

Sample	SiO_2[1] %	Al_2O_3[1] %	TiO_2[1] %	CaO[1] %	MgO[1] %	Na_2[1] %	K_2O %	Fe_2O_3t %	MnO[1] %	LOI %	Total %	S[1] %	CO_2[2] %	Au[3] ppb	As[4] ppm	Sb[5] ppm	Ag[4] ppm	Cu[4] ppm	Zn[4] ppm	Y[4] ppm	Zr[4] ppm	Sc[4] ppm	Cr[4] ppm	V[4] ppm	Ni[4] ppm	B[4] ppm
"Fresh" basalt (Balmer)																										
average (n=5)	50.60	15.00	1.01	10.6	6.88	2.58	0.19	12.55	0.20	0.6		0.21	0.12					106.0	109.5	21.5	67.1	38.2	249.67	290.2	113.4	
standard deviation	0.99	0.78	0.18	0.71	0.87	0.67	0.04	1.31	0.01	0.2		0.13	0.01					25.06	13.44	5.02	10.40	6.53	29.74		24.08	
Aluminous alteration (bleached basalt)																										
KG-01-090	78.32	14.60	0.98	0.21	0.21	0.07	1.26	1.04	0.01	1.4	98.47	0.09	< 0.18	11	479	34.9	0.4	195.0	9.1	2.2	21.0	9.9	50	141	373	27
KG-01-093	75.13	17.93	1.30	1.52	0.64	0.08	0.18	1.24	0.03	1.1	99.40	<	< 0.18	10	181	47.1	0.4	189.0	21.1	4.4	46.6	19.8	85	250	85	59
KG-02-003	79.70	14.05	1.03	0.20	0.08	0.05	0.39	0.56	0.00	1.2	97.56	0.04	< 0.18	42	154	12.7	0.7	261.0	8.5	3.8	35.6	5.3	44	108	75	42
KG-02-015	78.25	13.36	1.00	0.70	0.93	0.04	0.53	2.80	0.07	1.0	99.04	0.05	0.29	18	294	66.9	0.5	148.0	27.8	3.9	30.1	12.5	110	160	130	24
KG-02-030	79.33	13.79	1.09	0.32	0.46	0.04	0.24	2.28	0.03	1.5	99.36	0.01	< 0.18	2.5	138	38.6	0.4	175.0	24.5	3.6	32.4	10.4	90	151	91	23
KG-02-058	81.02	13.91	0.14	0.24	0.10	0.27	0.25	1.77	0.18	1.0	98.95	<	< 0.18	2.5	115	10.6	0.9	1.0	17.4	2.1	48.2	13.3	20	65	50	35
KG-02-079	81.29	12.44	0.72	0.22	0.18	0.07	0.55	1.76	0.01	1.4	99.01	0.14	< 0.18	20	219	39.3	<0.2	112.0	17.1	2.1	22.9	10.6	73	154	126	12
KG-01-109	62.05	18.12	1.38	1.85	1.57	0.97	4.16	2.78	0.03	3.8	97.31	0.31	0.94	21	333	15.8	0.4	257.0	52.1	6.7	70.3	56.7	79	386	104	801
KG-02-107	67.34	20.56	1.63	0.64	0.24	0.37	4.38	0.84	0.00	2.6	98.98	0.05	< 0.18	2.5	399	146.0	<0.2	262.0	227.0	3.7	63.4	36.4	78	372	182	179
KG-02-111	56.29	17.20	0.98	0.46	0.40	0.48	2.81	12.69	0.05	6.8	99.27	0.81	< 0.18	178	2700	44.0	1.2	25.4	11.3	3.4	38.1	36.1	118	322	148	51
KG-02-112	81.36	11.70	0.27	1.03	0.48	0.30	1.07	0.80	0.01	1.5	98.87	<	< 0.18	61	1500	41.1	<0.2	1.5	339.0	3.1	54.3	8.8	6	48	692	57
KG-02-118	80.47	15.45	0.40	0.12	0.18	0.08	0.20	1.39	0.03	1.2	99.95	0.09	< 0.18	26	1190	58.9	<0.2	30.6	326.0	3.8	106.0	4.7	17	48	490	117
KG-02-119	60.00	19.47	1.47	7.33	3.80	0.46	0.67	2.92	0.03	3.4	100.18	0.41	0.45	2.5	171	37.6	0.6	261.0	110.0	5.0	81.1	72.2	68	349	102	<10
KG-02-121	65.42	16.21	1.13	7.27	3.64	0.40	0.26	2.93	0.03	3.1	101.04	0.42	0.46	2.5	83	16.0	0.4	191.0	109.0	5.6	64.5	30.2	47	249	84	<10
KG-01-009	52.58	14.34	0.79	9.26	6.13	1.03	1.16	9.82	0.13	4.6	100.26	0.02	3.53	5	81	41.0	1.8	132.0	72.6	12.9	29.9	38.3	736	283	136	117
KG-02-048	71.65	15.65	0.97	1.71	1.81	0.28	1.02	5.65	0.08	2.1	101.52	0.12	0.29	6	269	51.3	0.7	120.0	36.8	3.9	35.4	38.0	1130	325	229	26
average	71.89	15.55	0.95	2.07	1.30	0.31	1.20	3.20	0.05	2.4	99.32	0.20	0.99	25.7	519.1	43.9	0.7	147.6	88.1	4.4	48.7	25.2	171.9	213.2	193.6	112.1
standard deviation	9.87	2.52	0.42	3.00	1.75	0.31	1.37	3.42	0.05	1.6	1.11	0.23	1.26	43.8	706.3	31.7	0.4	93.5	110.9	2.6	23.3	19.8	307.3	117.9	176.9	203.8
Garnet-magnetite altered basalt																										
KG-00-64	41.34	6.66	0.42	1.62	8.88	0.03	0.19	38.62	0.83	1.7	100.85	0.30	1.13	14	554	56.5	3.9	141.0	415.0	40.2	40.4	112.0	193	431	351	<10
KG-01-092	55.87	12.71	0.94	1.31	3.41	0.05	1.46	21.51	0.46	1.2	99.29	0.09	< 0.18	17	285	27.2	2.8	139.0	114.0	35.0	48.3	58.9	296	376	170	39
KG-01-101	60.35	12.38	0.93	3.12	4.45	0.17	0.54	15.77	0.34	2.3	100.73	0.07	< 0.18	37	745	26.6	1.4	73.6	75.3	8.2	26.9	26.8	190	198	212	122
KG-01-120	53.19	12.12	0.86	3.54	4.93	0.17	2.95	20.49	0.40	1.5	100.50	0.15	1.04	128	500	48.2	2.3	111.0	102.0	11.3	50.8	24.7	341	297	223	60
KG-02-020	40.66	10.32	0.72	5.92	7.21	0.15	0.76	31.88	0.73	1.9	100.73	0.24	2.53	200	350	34.0	3.9	50.7	276.0	63.1	53.0	92.2	251	426	213	27
KG-02-077	59.08	14.25	0.82	0.46	2.21	0.02	0.04	21.04	0.75	1.7	100.60	0.02	< 0.18	1400	150	27.2	2.5	180.0	84.8	15.0	39.4	41.2	234	324	93	21
KG-02-115	68.04	10.91	0.57	0.28	1.96	0.25	1.61	13.17	0.23	3.0	100.91	0.41	< 0.18	1380	4680	36.6	1.6	93.4	36.1	9.3	24.3	31.1	119	226	113	<10
KG-02-116	68.07	12.58	0.66	0.25	2.05	0.23	1.60	11.10	0.23	2.6	99.83	0.23	< 0.18	1490	1040	30.6	1.7	90.7	32.4	6.7	39.4	27.7	130	239	147	18
KG-02-023	31.81	4.69	0.33	1.99	8.12	0.03	0.02	50.06	1.14	0.7	99.59	0.36	1.51	59	626	91.3	5.5	50.0	1350.0	33.2	41.5	35.2	111	174	286	31
average	53.16	10.73	0.69	2.05	4.80	0.12	1.02	24.85	0.57	1.8	100.34	0.21	1.55	525	992	42.0	2.8	103.3	276.2	24.7	40.4	50.0	207	299	201	45.4
standard deviation	12.70	3.12	0.22	1.87	2.69	0.09	0.97	12.88	0.31	0.7	0.60	0.14	0.68	677	1408	21.1	1.4	43.9	421.8	19.4	9.8	31.7	81	97	82	36.5

[1]ICP by INRS-ETE. [2]Coulometry by XRAL laboratories. [3]Fire assay (gravimetric finish) by XRAL laboratories. [4]ICP by XRAL laboratories and ICP.AES by INRS-ETE. [5]Fusion/ICP/Hybrid AA by XRAL laboratories; LOI=loss on ignition

Table 2 (cont.)

Sample	SiO_2[1] %	Al_2O_3[1] %	TiO_2[1] %	CaO[1] %	MgO[1] %	Na_2O[1] %	K_2O[1] %	Fe_2O_3[1] %	MnO[1] %	LOI %	Total %	S[1] %	CO_2[2] %	Au[3] ppb	As[4] ppm	Sb[5] ppm	Ag[4] ppm	Cu[4] ppm	Zn[4] ppm	Y[4] pp	Zr[4] ppm	Sc[4] ppm	Cr[4] ppm	V[4] ppm	Ni[4] ppm	B[4] ppm
Carbonate-magnetite breccia																										
KG-01-013	19.70	0.88	0.05	6.23	12.51	0.01	0.02	43.14	1.21	14.5	100.7	2.26	8.26	913	157	41.7	5.4	149.0	612.0	6.6	24.3	54.3	34	239	145	<10
KG-01-029	20.89	2.27	0.16	16.01	13.17	0.02	0.02	23.42	0.50	22.3	100.2	0.82	15.74	1190	6000	62.8	3.2	56.6	269.0	9.6	17.9	26.1	58	134	81	13
KG-02-020	34.88	4.14	0.27	7.36	9.11	0.03	0.05	37.32	0.95	6.61	102.0	1.12	7.17	5900	707	44.9	5.5	119.0	689.0	34.	29.1	65.4	89	284	277	<10
KG-02-064	11.42	0.46	0.02	20.48	12.35	0.01	0.01	24.95	0.53	25.7	97.48	1.40	20.87	1270	41	25.9	3.2	130.0	73.5	8.5	17.3	60.9	29	130	95	<10
average	21.72	1.94	0.13	12.52	11.78	0.02	0.03	32.21	0.80	17.3	100.1	1.40	13.01	2318	1726	43.8	4.3	113.7	410.9	14.	22.2	51.7	53	197	150	-
standard deviation	9.73	1.66	0.11	6.88	1.82	0.01	0.02	9.59	0.34	8.54	1.93	0.62	6.48	2393	2864	15.1	1.3	40.0	289.7	13.	5.6	17.6	27	77	89	-
Biotite-carbonate altered basalt																										
KG-00-10 (weak alt.)	59.67	13.95	0.98	7.86	5.32	0.20	1.15	10.33	0.18	2.52	102.6	0.19	1.48	22	576	45.6	1.5	150.0	95.0	13.	44.0	34.8	261	315	167	<10
KG-02-016 (weak alt.)	32.57	10.94	0.69	12.03	6.17	0.53	2.01	19.22	0.18	12.4	99.75	2.84	8.65	402	147	21.4	4.0	172.0	64.7	6.9	46.2	28.1	120	64	148	<10
KG-00-016 (deformed)	55.33	12.97	0.95	10.29	4.95	0.17	0.79	8.35	0.18	6.30	100.7	0.21	5.24	27	420	20.1	1.0	131.0	55.7	12.	39.3	37.5	229	275	219	<10
KG-01-033	53.76	10.24	0.76	9.30	4.49	0.18	1.86	8.28	0.15	9.52	100.9	1.54	6.52	4350	8540	70.6	4.3	43.1	69.2	8.0	35.2	33.9	140	326	209	11
KG-01-097	41.54	8.97	0.61	12.85	6.91	0.25	1.90	10.28	0.23	14.5	100.5	2.08	13.58	1590	1940	38.4	3.2	86.6	86.5	8.1	31.3	29.6	104	200	155	81
KG-01-099	50.51	10.82	0.92	10.67	4.64	0.16	2.29	9.95	0.13	9.50	101.8	1.63	6.85	2840	5360	80.7	1.9	170.0	249.0	8.1	54.6	17.4	96	267	107	38
average	48.90	11.31	0.82	10.50	5.41	0.25	1.67	11.07	0.17	9.13	101.0	1.41	7.05	1539	2831	46.1	2.7	125.5	103.4	9.6	41.8	30.2	158	241	168	43
standard deviation	10.05	1.83	0.15	1.81	0.95	0.14	0.57	4.10	0.03	4.29	1.01	1.05	4.00	1759	3402	25.1	1.4	51.1	72.8	2.9	8.3	7.2	70	98	41	35
Arsenopyrite replacement zones																										
KG-00-35 (basalt)	52.35	11.16	0.83	7.38	3.94	0.18	2.05	11.10	0.09	7.94	100.4	1.45	3.48	8500	18083	91.5	2.4	119.0	106.0	6.8	48.0	29.7	128	272	107	<10
KG-01-102 (basalt)	50.50	12.65	0.94	8.76	4.28	0.28	1.81	12.46	0.17	6.66	101.8	1.40	3.93	3920	16114	73.9	4.5	454.0	101.0	6.7	42.3	35.4	195	263	177	59
KG-02-060 (basalt)	55.55	12.04	0.86	8.36	4.08	0.24	2.05	8.53	0.13	7.66	101.7	0.98	4.08	8600	10328	142.0		111.0	69.9	7.0	39.9	34.5	165	291	149	58
KG-02-067 (komatiite)	69.15	5.00	0.40	2.63	1.66	0.08	1.46	7.81	0.04	9.14	101.6	0.58	2.58	44400	31338	1820		157.0	2250.0	1.4	16.6	11.8	106	818	640	45
average	56.89	10.21	0.76	6.78	3.49	0.19	1.84	9.98	0.11	7.85	101.4	1.10	3.52	1635	18966	531.9	3.5	210.3	631.7	5.5	36.7	27.9	387	411	268	54
standard deviation	8.44	3.53	0.24	2.83	1.23	0.09	0.28	2.18	0.06	1.02	0.64	0.41	0.67	1882	8880	859.3	1.5	163.7	1079.0	2.7	13.8	11.0	450	272	249	8
Basaltic komatiite (biotite-carbonate altered)																										
KG-00-84A	44.38	3.19	0.18	15.67	7.32	0.10	0.67	7.08	0.19	20.6	100.3	0.53	17.46	411	1300	20.0	1.1	26.1	29.8	4.5	8.0	15.5	781	91	605	19
KG-00-84B	39.11	5.87	0.42	15.28	6.82	0.17	1.37	10.32	0.14	19.5	101.4	1.60	15.52	963	1970	27.3	1.6	64.6	62.7	5.2	15.9	27.5	204	181	113	15
average	41.75	4.53	0.30	15.48	7.07	0.13	1.02	8.70	0.17	20.1	100.8	1.07	16.49	687	1635	23.7	1.4	45.4	46.3	4.9	12.0	21.5	141	136	868	17
standard deviation	3.73	1.90	0.17	0.28	0.35	0.05	0.50	2.29	0.04	0.74	0.79	0.76	1.37	390	474	5.2	0.4	27.2	23.3	0.5	5.6	8.5	890	64	371	3

[1]ICP by INRS-ETE. [2]Coulometry by XRAL laboratories. [3]Fire assay (gravimetric finish) by XRAL laboratories. [4]ICP by XRAL laboratories and ICP-AES by INRS-ETE. [5]Fusion/ICP/Hybrid AA by XRAL laboratories; LOI=loss on ignition

1% loss on ignition, and a ratio of cation Al/(Na+K+Ca) or peraluminous index of approximately 1 indicating little alkali bulk leaching (Table 2).

Aluminous alteration (bleached basalt)

Penczak and Mason (1999) presented the aluminous alteration as a zoned alteration derived from a metamorphosed and recrystallized early hydrothermal alteration. This alteration corresponds to the earliest of the four episodes described by Tarnocai (2000). It produced an assemblage of andalusite-chloritoid-white mica-margarite-garnet in the amphibolite-facies domains.

Bleaching occurs preferentially in tholeiitic variolitic flows at the Campbell and Red Lake mines. In the High Grade zone, bleached basalts are present as beige metre-wide replacement zones (Fig. 2a). These zones are usually variolitic and show evidence of pillows with darker rims of chlorite. The varioles are lighter beige than the host bleached basalt. In core, bleaching occurs as medium grey-coloured zones.

According to our underground observations, no direct spatial relationship exists between bleaching and high-grade ore zones. There is no evidence that the aluminous alteration was a zoned envelope around ore pods that was later disrupted by faulting. However, the bleaching could be associated with the gold-rich hydrothermal system, but at a scale too large for this relationship to be easily appreciated.

The mineralogical assemblage defined for this alteration is andesine-sericite-biotite-chlorite-quartz-andalusite-staurolite±garnet±epidote± chloritoid. Bleached basalts generally contain 30% of quartzofeldspathic matrix in which plagioclase (andesine) is more or less altered to sericite. Varioles are filled with very fine grained material composed of quartz and aluminosilicates (andalusite and/or staurolite; Fig. 2b, c). Andalusite and staurolite also occur as coarse crystals both in the varioles and matrix (Fig. 2d); they show irregular margins and often a blurred aspect. Idiomorphic andalusite contains aligned inclusions that show evidence of rotation, indicating that andalusite is syn- to late-deformational (Fig. 2d). Andalusite and staurolite are deformed, which suggests they have at least been affected by the latest deformation. These minerals are also present in host-rock enclaves within quartz veins that crosscut the fabric. The samples of bleached basalt also contain up to 25% quartz±biotite±chlorite±andalusite±sulphide veins. Quartz is coarse-grained and shows a rolling

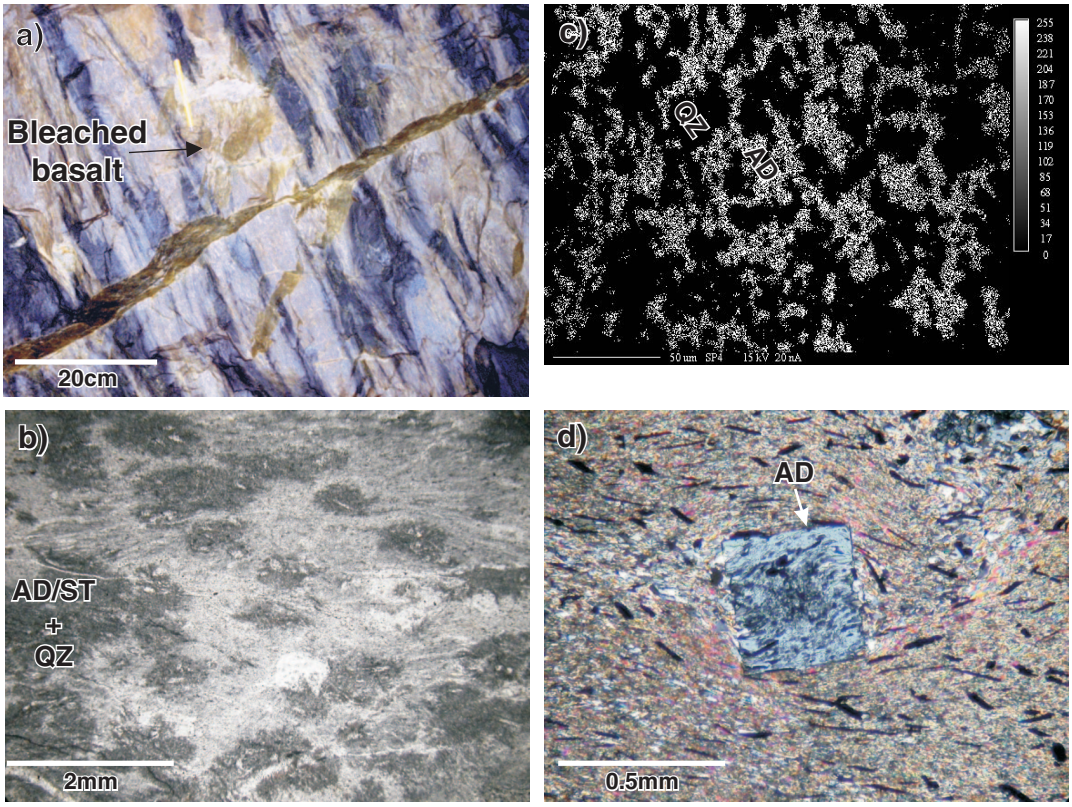

Figure 2. a) Aluminous alteration affecting variolitic and pillowed Balmer basalt, section view; **b**) photomicrograph showing andalusite (AD), quartz (QZ), and staurolite (ST) in the aluminous alteration zone; **c**) microprobe photograph of andalusite (AD) and quartz (QZ); **d**) photomicrograph of andalusite (AD, indicated by arrow) with aligned inclusions which are themselves affected by the deformation.

extinction, which indicates it was affected by at least the latest deformation. Quartz is also found in pressure shadows of andalusite crystals, and in clusters and disseminated in the matrix. Biotite and chlorite are mainly associated with quartz veins. Biotite is usually brownish red (ferriferous, Fig. 3; mean Mg:Fe ratio = 0.64), sometimes light to medium brown (more magnesian, Fig. 3; mean Mg:Fe ratio = 1.35), mainly concentrated along and within quartz veins, but also disseminated as small clusters in the matrix. Chlorite has a ripidolite composition and is mainly concentrated along quartz veins, and in bands and disseminated between the varioles. Almandine-rich garnet (with a spessartite component), epidote, and chloritoid are locally present.

Two samples (KG-02-115B and KG-02-116B) that may be transitional between the aluminous and the garnet-magnetite alteration contain 3 to 5% garnets, aluminosilicates and epidote (along with chlorite, quartz, and sericite). One sample contains nearly 20% poikilitic andalusite associated with garnet and staurolite. Staurolite (5%) occurs as poikilitic idiomorphic to irregular crystals. Epidote is either associated with opaque minerals or in inclusions within garnets.

Sulphide minerals are disseminated and in aggregates both in the matrix and in quartz veins. Opaque minerals form 1 to 20% of these rocks. Pyrite is the main sulphide mineral and counts for up to 15% of the mineral content. Pyrite is occasionally associated with pyrrhotite, and chalcopyrite is locally present. Gersdorffite and ullmannite were identified by microprobe analyses. Finely disseminated magnetite is frequently observed and ilmenite is found locally.

The development of aluminosilicate minerals in mafic precursors requires that the rocks experienced pervasive chemical alteration either prior to, or coincidental with, the peak of metamorphism (Andrew et al. 1986; Dubé et al. 2000). Penczak (1996) and Damer (1997) interpreted the aluminous alteration as an early hydrothermal event characterized by leaching of alkalis, especially Na. Penczak and Mason (1999) also described the bleached zone as depleted in Ca, Na, Fe, Mg, and Mn. They mentioned that this alteration is genetically linked with the garnet alteration, which is characterized by an addition of Fe and Mn. They also reported that both aluminous and garnet alterations were enriched in Si. Our analyses (Table 2) show that the average Al_2O_3, TiO_2 and Zr contents of this alteration are similar to those of the least altered basalts and define an isocon (Fig. 4A). The average composition of the bleached basalts indicate that they are strongly leached in CaO, $Fe_2O_3^t$, MgO, MnO and Na_2O (Fig. 4A), whereas they are significantly enriched in SiO_2, and K_2O. Three samples have a very low TiO_2 content

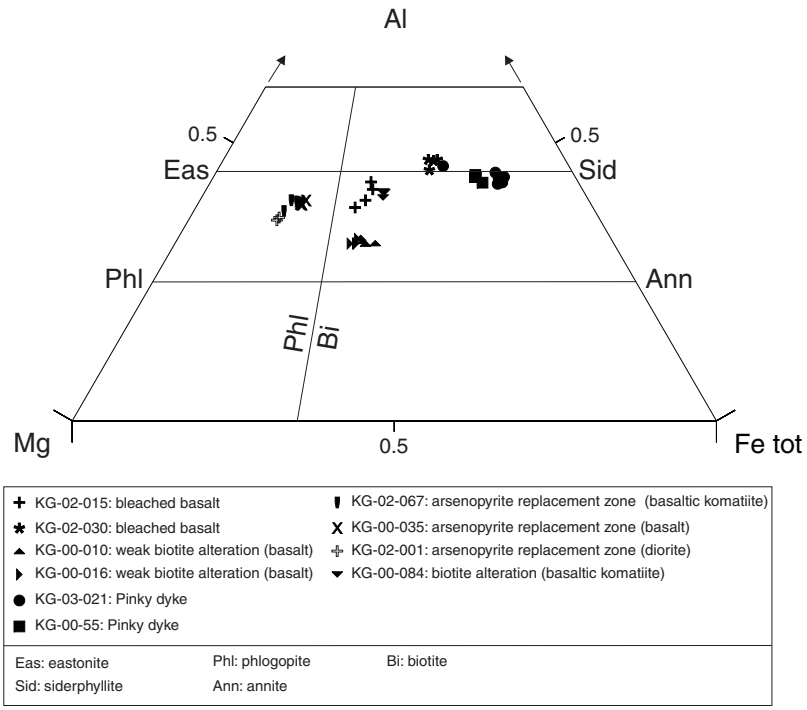

Figure 3. Biotite composition, biotite (Bt) and phlogopite (Phl) form a solid-solution series and the terminology is arbitrary. The boundary between these two minerals is set according to a ratio Mg:Fe > 2:1 for the phlogopite.

(KG-02-058, KG-02-112, and KG-02-118), partly explained by their very high SiO_2 content due to small quartz clusters and veinlets. Samples from this alteration type are barren (5 to 61 ppb), to anomalous in Au (178 ppb), and some contain elevated values in As (≤2700 ppm), Cu (≤262 ppm), and Zn (≤339 ppm) (Table 2).

Garnet-magnetite alteration

Damer (1997) described the garnet alteration as a distal zone characterized by chlorite-plagioclase-garnet-andalusite- quartz-staurolite-chloritoid-biotite-ilmenite±cummingtonite. Penczak and Mason (1999) presented the garnetiferous zone as a distal alteration facies derived from -metamorphosed and recrystallized hydrothermal alteration. This alteration type corresponds to the assemblage observed by Tarnocai (2000) in rocks of the amphibolite-facies domains adjacent to the gold veins and containing biotite-amphibole-garnet-plagioclase.

The exact relationship between the garnet-magnetite assemblage and the ore is difficult to establish. Detailed mapping of the ramp on level 37 has shown irregularly distributed garnet- and magnetite-rich zones without any clear association to known ore zones, suggesting that the garnet-magnetite assemblage may be mainly linked to the regional medium-grade metamorphism. Locally, however, the garnet-magnetite assemblage is in close spatial association with some high-grade ore zones, where it forms an external halo to the biotite-sulphide alteration zone. Elsewhere, high-grade ore zones, such as the Hangingwall shear on level 34, gradually become lower grade magnetite-rich zones along strike.

The assemblage consists of variable proportions of garnet-carbonate minerals-chlorite-biotite-amphibole±plagioclase±chloritoid±andalusite±staurolite±epidote. Garnets in this assemblage are almandine-rich (with a spessartite or grossular component), and count for 1 to 40 vol %. They are light pink, coarse grained, poikilitic, and Mn-rich. They are either hypidiomorphic (Fig. 5a) or have a granulated aspect and irregular recrystallized margins (Fig. 5b). They contain aligned inclusions and are locally affected by the deformation (stretched and rolled-up crystals; Fig. 6a, b, c), which implies they are syndeformational. Carbonate minerals (ankerite and ferrodolomite) are found in multiple crosscutting injections. Two types of chlorite are associated with the carbonate minerals: ripidolite and diabantite. The biotite proportion varies significantly in these samples from 0 to 55 vol %. The colour of biotite also changes from light or medium brown to greenish or reddish brown. Biotite is usually allotriomorphic and disposed in bands marking the foliation along with chlorite and amphiboles. Amphiboles are of two types: cummingtonite and alumino-ferro-tschermakite. Cummingtonite is more common. It is either in clusters of parallel or radiating fibres, in veins with quartz and carbonate minerals, or in tails of rolled-up garnets. Alumino-ferro-tschermakite is generally acicular, bluish green, associated with biotite or in layers with quartz, plagioclase, biotite, and chlorite. Plagioclase relicts are common. These plagioclase crystals are cut and replaced by garnet and chlorite. Chloritoid (5 vol %) occurs locally.

The opaque mineral assemblage is composed of magnetite-pyrrhotite-arsenopyrite±pyrite±pentlandite±gold±ilmenite. Magnetite (15–30 vol %) is the main opaque mineral. It is usually disseminated or associated with sulphide minerals,

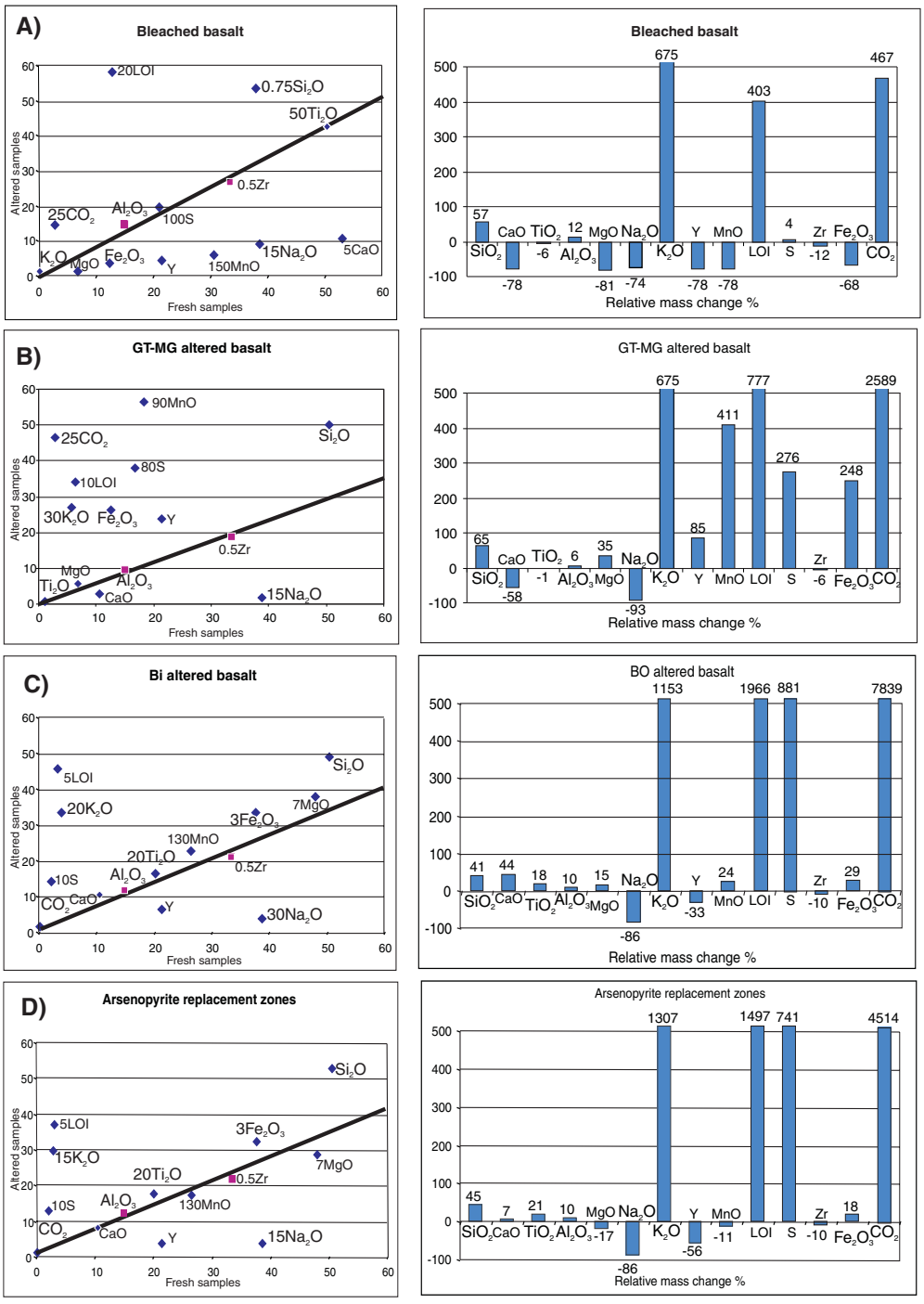

Figure 4. Isocon diagrams (according to Grant=s method, 1986) and histograms (according to Huston, 1993) illustrating relative mass changes for altered rocks of the different facies compared to 'fresh' Balmer assemblage basalts. Based on average composition of basalts only (Table 2). Isocons are shown according hypotheses of constant alumina and zirconium. Net mass changes (ΔMA) relative to the least-altered equivalent are estimate as follows: ΔMA = 100 (1/m-1) where m is the slope. Multiple factors used for clarity.

and locally occurs in garnet cores and at the margins of garnet crystals. Magnetite contains pyrrhotite, pyrite, and arsenopyrite inclusions, which implies that, at least locally, it formed later than these minerals. Pyrrhotite is present as small aggregates with magnetite± arsenopyrite±pyrite. Both pyrrhotite and magnetite are present as inclusions in garnet and andalusite. Pyrrhotite contains pyrite and arsenopyrite inclusions along with pentlandite exsolutions. Arsenopyrite is found in most samples in aggregates with pyrrhotite±magnetite or disseminated. Half of the samples contain pyrite that is disseminated and in aggregates with the other sulphide minerals and magnetite, or in quartz veinlets. Locally, pyrite inclusions in garnet and andalusite contain inclusions of magnetite. Traces of gold locally occur as free grains or in arsenopyrite.

Figure 4B shows that the average TiO_2, Al_2O_3 and Zr contents define an isocon indicating that these elements were relatively stable. However, the TiO_2 content is anomalously low in three samples. CaO and Na_2O are strongly leached, whereas $Fe_2O_3^t$, MnO, K_2O, S, and CO_2 are enriched. The

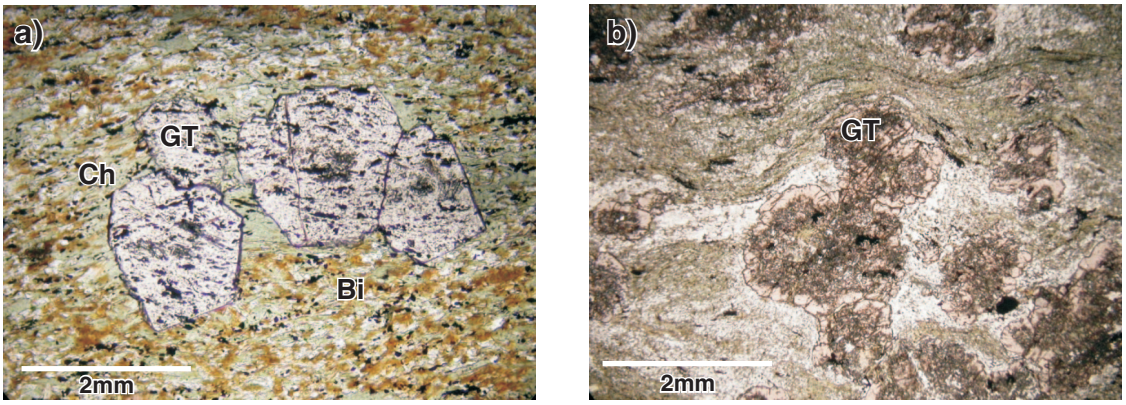

Figure 5. a) Photomicrograph showing hypidiomorphic garnets (GT) in the garnet-magnetite alteration zone (Ch - chlorite, Bi - biotite); **b**) photomicrograph of garnet (GT) with granulated aspect and irregular margins.

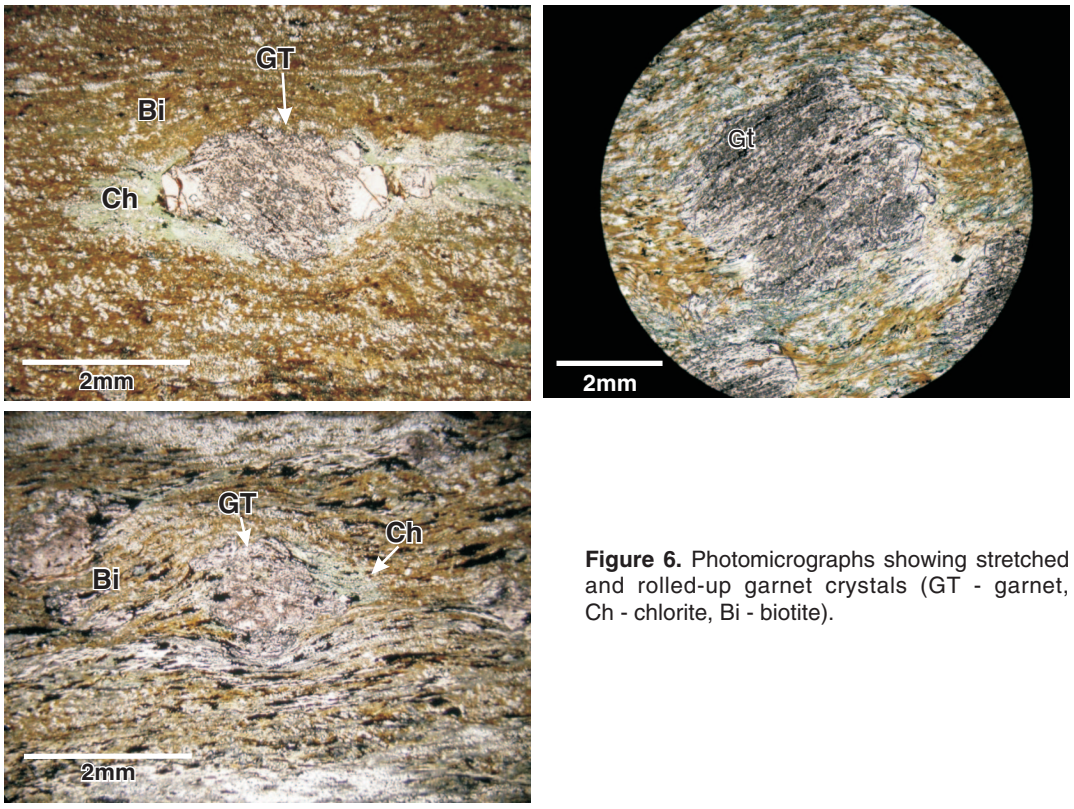

Figure 6. Photomicrographs showing stretched and rolled-up garnet crystals (GT - garnet, Ch - chlorite, Bi - biotite).

samples from this zone also show a high loss on ignition. Locally, Zn shows relatively high concentration (up to 1350 ppm, Table 2). Samples from this type of alteration returned up to 1490 ppb Au and 4680 ppm As.

Carbonate breccias and overprinting carbonate-magnetite breccias

The carbonate breccias correspond to the main-stage phase described by Penczak and Mason (1999) as barren colloform-crustiform carbonate and quartz veins, cockade breccias, and sheeted to stockwork veinlet zones crosscutting the early alteration. The formation of these breccias corresponds to the second episode of fracturing and hydrothermal alteration described by Tarnocai (2000). It produced an iron carbonate pervasive alteration with carbonate and quartz-carbonate veinlets as well as chloritization destroying the original mineralogy of the basalt. Penczak (1996) and Damer (1997) also described an episode of post-bleaching quartz-carbonate veining and brecciation.

There are numerous carbonate veins and breccia veins within the High Grade zone (Dubé et al., 2001). The relationship between carbonate veins and magnetite is complex. The carbonate breccia veins are commonly overprinted by hydrothermal magnetite distributed in the veins or along their margins (Fig. 7), whereas local crustiform carbonate veins contain conformable bands of magnetite or cut magnetite-rich breccias. Semi-massive magnetite alteration is also found in association with late brittle-ductile faults in the High Grade zone, but the relationship between this magnetite and the overprinted magnetite alteration is unclear. In places, millimetre- to centimetre-thick magnetite-rich faults with subhorizontal slickenlines (e.g. 37-776-1 stope, sill cut) clearly cut through high-grade ore zones, whereas elsewhere, auriferous arsenopyrite-rich replacement zones clearly overprint and replace carbonate-magnetite breccia veins. These relationships suggest more than one stage of hydrothermal magnetite and/or remobilization.

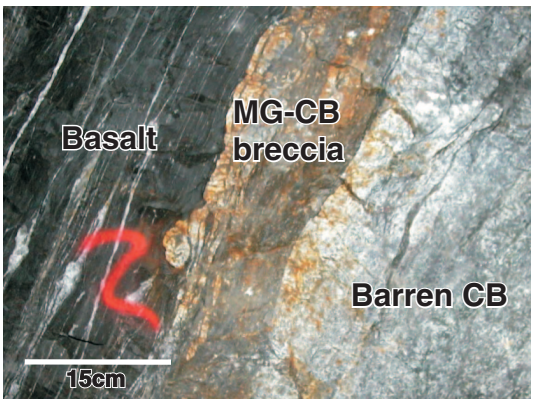

Figure 7. Carbonate-magnetite breccia showing clasts of iron carbonate vein in a magnetite-rich matrix developed along the wall of a barren iron- carbonate vein, section view (CB - carbonate, MG - magnetite).

In the High Grade zone, the carbonate breccias generally consist of carbonate-plagioclase-chlorite-cummingtonite± hornblende±quartz. Carbonate (ankerite) constitutes 35 to 75 vol % of the mineralogical assemblage, forming veins and clusters. The samples are brecciated and carbonate injections are numerous and crosscut one another. Altered plagioclase is interlayered with mafic minerals and is derived from incorporated wall-rock clasts. Quartz is locally observed in rounded clusters among carbonate minerals or in thin layers parallel to the foliation. Chlorite (ripidolite) is in clusters of radiating fibres or associated with biotite clusters. Clusters of cummingtonite (anthophyllite) are found in association with chlorite or carbonate minerals (Fig. 8a, b). Hornblende is locally present and is replaced by chlorite and carbonate minerals.

Opaque minerals form 10 to 25 vol % of the carbonate-magnetite breccias. Magnetite and pyrrhotite are found in aggregates in all samples and contain inclusions of each another. Where the contact with the host rock is exposed, magnetite has two different habits: finely disseminated in the host rock; and, in the breccia, crystals are coarser and associated with sulphide minerals. Arsenopyrite in aggregates with magnetite and pyrrhotite was locally observed. This arsenopyrite formed relatively late because it contains inclusions of magnetite and pyrrhotite.

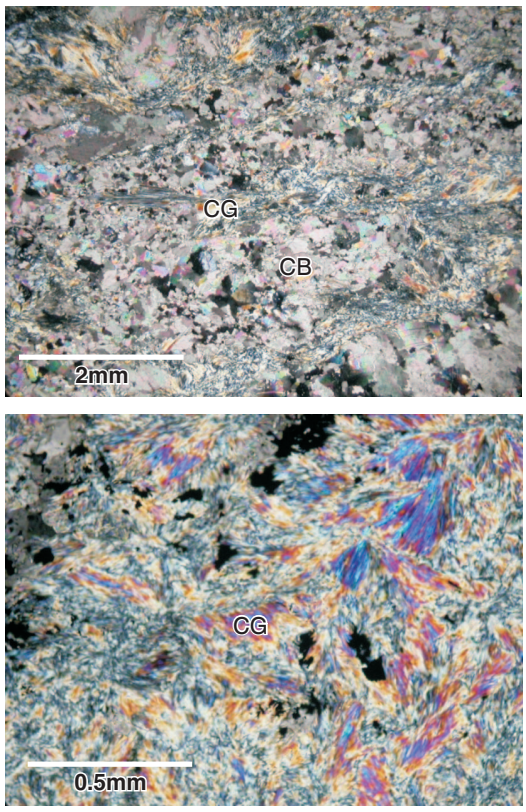

Figure 8. Photomicrographs showing clusters of cummingtonite (anthophyllite) (CG) found in association with chlorite or carbonate (CB).

The carbonate-magnetite breccia samples contain little Al_2O_3, Na_2O, K_2O and TiO_2. However, they contain high amounts of CaO, $Fe_2O_3{}^t$, MgO, MnO, CO_2 and some S, and have a very important loss on ignition. The breccia samples contain an average of 2320 ppb Au, up to 6000 ppm As, and local anomalously high Zn concentrations (Table 2).

Biotite-carbonate alteration

The carbonatization and pervasive biotite (potassic) alteration are part of the early alteration phase and this occurs proximal to alteration-controlling structures in highly carbonatized and/or silicified rocks (Damer, 1997; Penczak and Mason, 1999). The biotite-carbonate alteration type corresponds to the third fracturing and hydrothermal alteration episode linked to the gold mineralization described by Tarnocai (2000).

Within the High Grade zone, the biotite-carbonate alteration in basalts commonly forms an envelope surrounding the gold-bearing silicic replacement and arsenopyrite-rich zones. The latter are usually within or along the margins of carbonate veins or forming an alteration front replacing the altered basalt. However, biotite-carbonate alteration can also be related to higher strain deformation zones, whether or not they are associated with gold mineralization and silica-arsenopyrite replacement. The biotite-carbonate altered zones are commonly very well foliated within the High Grade zone (Fig. 9). This suggests that biotite is pre- to syn-deformational.

The mineralogical assemblage consists of biotite-anorthite-amphiboles-carbonate minerals. Biotite (slightly magnesian biotite; Fig. 3) is light brown and forms 15 to 30 vol % of the mineralogical assemblage. The biotite forms bands delineating the schistosity in the matrix and along, or within, carbonate-quartz veins, where it is coarser, idiomorphic, and slightly darker. Biotite layers are cut by carbonate and sulphide minerals. Highly altered plagioclase (anorthite) is the principal mineral of the matrix; it is replaced by sericite, biotite, and carbonate minerals. Three types of amphiboles are present in the least-altered samples: dark green ferro-magnesian hornblende associated with light green sub-calcic ferro-magnesian hornblende that are both cut by cummingtonite. Carbonate minerals (calcite, ankerite, and ferro-dolomite) are found in veins, alone or with quartz-biotite-muscovite-sulphide minerals, and in the matrix, as pervasive alteration.

Biotite-altered basalts contain 10 to 20 vol % sulphide minerals accompanied by some oxide minerals (up to 2 vol %). The main sulphide minerals are arsenopyrite, pyrite, and pyrrhotite, which are disseminated and in aggregates both in the matrix and quartz-carbonate veins. Magnetite and rutile are locally present, as finely disseminated grains along the schistosity.

Figure 4C shows that Al_2O_3 and Zr are relatively stable and define an isocon. Biotite-altered basalts are strongly leached in Na_2O and contain less Y. They are significantly enriched in K_2O, CO_2, and S with some gains in SiO_2, CaO and Fe_2O_3. They show a higher loss on ignition than relatively fresh basalts (Fig. 4C). This alteration type is associated with the gold mineralization. Except for two weakly altered samples (KG-00-10, KG-02-16) and one highly deformed sample (KG-00-16), all returned more than 1500 ppb Au and significant As concentrations (Table 2).

Arsenopyrite-rich replacement zones

Within the High Grade zone, arsenopyrite-rich replacement zones are associated with very high-grade ore zones. Arsenopyrite-rich replacement is common along the margins and within silicified carbonate veins, or forming structurally controlled arsenopyrite-rich zone replacing the Balmer basalt with only local evidence of carbonate-quartz veins or clasts. The arsenopyrite-rich replacement zones are commonly surrounded by a biotite-carbonate alteration envelope (Fig. 10).

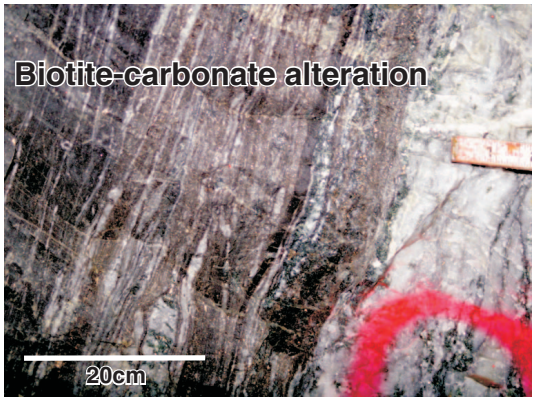

Figure 9. Section view showing reddish-brown biotite-carbonate alteration zone along the selvage of a high-grade quartz-carbonate vein.

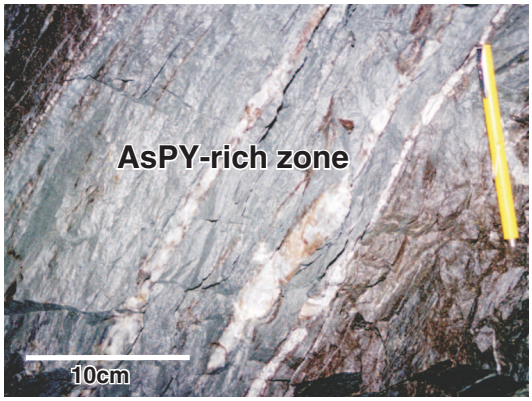

Figure 10. Arsenopyrite-rich (AsPY) high-grade auriferous replacement zone, section view.

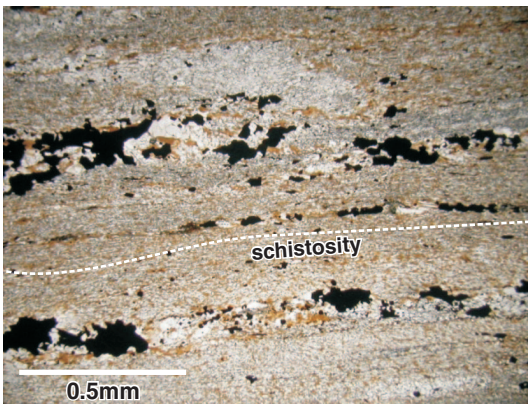

Figure 11. Photomicrograph showing biotite (phlogopite) that marks the foliation.

Some arsenopyrite-rich replacement zones are also found in the basaltic komatiite (sample KG-02-67; Table 2) and locally in diorite.

The mineralogical assemblage of this alteration type is similar to the biotite-carbonate alteration, except for its high arsenopyrite content, and consists of biotite-plagioclase-carbonate minerals-quartz-sericite. In addition to these minerals, some fuchsite is disseminated in the basaltic komatiite. Biotite (phlogopite composition; Fig. 3) is light brown and forms 15 to 40 vol % of the mineralogical assemblage. In the matrix, the biotite is layered and marks the schistosity (Fig. 11). It can also be observed along and within carbonate-quartz veins (coarser, idiomorphic, and slightly darker). Highly altered plagioclase constitutes the main mineral of the matrix where it is replaced by sericite, biotite, and carbonate minerals. The carbonate minerals (calcite and ankerite) are found in veins, with or without quartz-biotite-muscovite-sulphide minerals, and in the matrix as pervasive alteration.

Arsenopyrite-rich replacement zones contain 10 to 20 vol % sulphide minerals with traces of visible gold and oxide minerals (magnetite, ilmenite). The main sulphide minerals are arsenopyrite, pyrite, and pyrrhotite which are disseminated and in aggregates both in the matrix and quartz-carbonate veins.

Arsenopyrite-rich replacement zones hosted by the basalt have a composition similar to that of biotite-carbonate-altered samples. Figure 4D shows that Al_2O_3 and Zr define an isocon. They are strongly leached in Na_2O and contain less Y than their precursor. They are significantly enriched in K_2O, S, and CO_2 with some gains in SiO_2 (Fig. 4D). They show a higher loss on ignition than relatively fresh basalts. The arsenopyrite-rich replacement zones represent the ore zones and this is reflected by the analytical results between 3920 and 44400 ppb Au and high As contents with local elevated concentration of Sb and Zn (Table 2).

DISCUSSION

The mineralogical assemblages defined in this study support the fact that the rocks are at the greenschist-amphibolite-facies transition. Chlorite occurs in several alteration facies, but the rest of the assemblage is more characteristic of amphibolite facies. The limit between the greenschist and amphibolite facies in the metamorphosed basalts of the Red Lake belt is gradual and results in a transitional zone (Thompson, 2003). The assemblage actinolite-epidote-chlorite-albite is diagnostic of greenschist-facies rocks (Thompson, 2003). Hornblende appears in basalts with an increase of metamorphic degree. Rocks containing both hornblende and actinolite with lesser quantities of chlorite or epidote are diagnostic of the transition zone. The basalt considered in the current study do not contain actinolite, but contain tschermakite, hornblende, cummingtonite, and anthophyllite, and are compatible with such a transitional zone and thus re-emphasize the exploration potential proposed by Thompson (2003). All alteration types contain chlorite except for the biotite-carbonate alteration and arsenopyrite-rich replacement. The lack of chlorite in both these zones supports the zonation defined by Damer (1997) and Penczak and Mason (1999) who described a grade outward from biotite-rich domains to more chlorite-rich domains and a chlorite overprint on biotite.

Thompson (2003) mentioned that the mineralogical assemblages of volcanic rocks, which were affected by an early aluminous alteration, are related to later regional metamorphism. The characteristic assemblage of the aluminous alteration at the greenschist facies varies from chlorite-white mica, to chloritoid-chlorite, to biotite-garnet-chlorite. At the amphibolite facies, it is composed of staurolite-andalusite-biotite, cordierite-andalusite-biotite, or cordierite-orthoamphibole. In this study, the andalusite-chloritoid, andalusite-staurolite, and orthoamphibole-garnet-chlorite-andalusite-staurolite assemblages were identified. Such alteration assemblages are compatible with metamorphosed argillic and advanced argillic alterations due to acid leaching by low pH fluids. However, the possible

Figure 12. Aluminous altered pillow basalt cut by barren iron carbonate vein and then flattened, 37-756-1 Stope access, Red Lake mine (AD - andalusite).

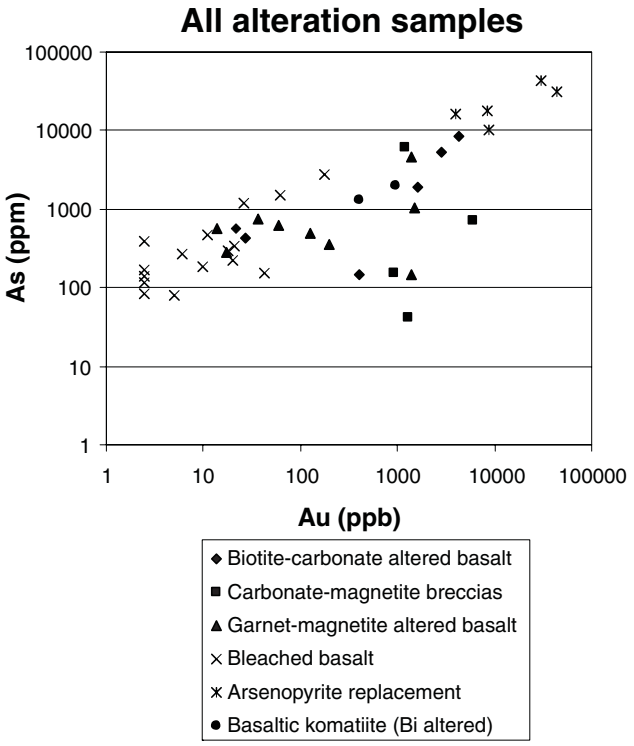

Figure 13. Diagram showing As vs Au in the various alteration zones.

genetic relationship between this leaching and the ore remains to be better defined. Locally, the aluminous bleaching is cut by a deformed colloform-crustiform iron-carbonate vein (Fig. 12). This chronological relationship suggests that the aluminous alteration is very early stage and clearly pre-mineralization.

The majority of the minerals in the alteration assemblages described are syn-deformational. Some carbonate veins cut all assemblages. Other carbonate veins, however, are folded and faulted, indicating they were affected by deformation. Dubé et al. (2003) established several stages of carbonatization within the Red Lake mine trend and stated that evidence from the Red Lake mine supports such a protracted multistage event with pre-, early and late to post-deformation iron-carbonate veining.

The biotite-carbonate alteration and the arsenopyrite replacement zones are clearly associated with the gold mineralization (Table 2). In fact, except for two weakly altered and one strongly deformed samples, all samples of these alteration types returned more than 1500 ppb Au (Table 2). Figure 13 illustrates an overall Au-As positive correlation. The majority of the mineralized samples, from all alteration types, contain magnesian biotite (Fig. 3). However, three samples of garnet-magnetite-altered basalt that contain a more ferriferous biotite graded 1400 ppb Au (Table 2). The presence of magnesian biotite can help distinguish biotite assemblages associated with gold mineralization from biotite zones unrelated to ore.

All alteration assemblages show a lower Na_2O and a significantly higher K_2O content than relatively fresh basalts and may represent a first-order footprint of the mineralization. For the other elements, changes vary from one facies to another. The biotite-carbonate alteration and the arsenopyrite-rich replacement zones show net mass gain due to an increase in K_2O, S, CO_2 and SiO_2 compared to 'fresh' basalts that could be used with Au and As as a geochemical signature for the proximal alteration zone.

The mineralogical assemblages and the lithogeochemistry of the High Grade zone at the Red Lake mine support the interpretation of MacGeehan and Hodgson (1982) and Dubé et al. (2003) according to which the Campbell-Red Lake deposit is a complex metamorphosed and deformed deposit that represents the end product of several stages of hydrothermal alteration and gold mineralization. The size and grade of the Campbell-Red lake deposit are probably related, at least in part, to this complexity.

ACKNOWLEDGMENTS

The Goldcorp Inc. Red Lake Mine, in particular Gilles Filion, Stephen McGibbon, Rob Penczak, the late John Kovala, and the entire production staff are thanked for their scientific contribution, logistical and financial support, critical review and permission to publish. We benefited from discussions with Jack Parker of the Ontario Geological Survey. The Ontario Geological Survey and its regional office in Red Lake are thanked for their support and collaboration. We acknowledge the NSERC, which has provided a grant through a partnership agreement with the Earth Sciences Sector of Natural Resources Canada and Goldcorp Inc.

REFERENCES

Andrews, A.J., Hugon, H., Durocher, M., Corfu, F., and Lavigne, M.J.
1986: The anatomy of a gold-bearing greenstone belt: Red Lake, northwestern Ontario, Canada; *in* Proceedings of Gold '86, an International Symposium on the Geology of Gold Deposits, (ed.) A.J. Macdonald; Geological Association of Canada, p. 3–22.

Christie, B.J.
1986: Alteration and gold mineralization associated with a sheeted veinlet zone at the Campbell Red Lake mine, Balmertown, Ontario; M.Sc. thesis, Queen's University, Kingston, Ontario, 334 p.

Damer, G.C.
1997: Metamorphism of hydrothermal alteration at the Red Lake mine, Balmertown, Ontario; M.Sc. thesis, Queen's University, Kingston, Ontario, 195 p.

Dubé, B., Balmer, W., Sanborn-Barrie, M., Skulski, T., and Parker, J.
2000: A preliminary report on amphibolite-facies, disseminated-replacement-style mineralization at the Madsen gold mine, Red Lake, Ontario; Geological Survey of Canada, Current Research 2000-C17, 12 p.

Dubé, B., Williamson, K., and Malo, M.
2001: Preliminary report on the geology and controlling parameters of the Goldcorp Inc. High Grade zone, Red Lake mine, Ontario; Geological Survey of Canada, Current Research 2001-C18, 23 p.
2002: Geology of the Goldcorp Inc. High Grade zone, Red Lake mine, Ontario: an update; Geological Survey of Canada, Current Research 2002-C26, 13 p.
2003: Gold mineralization within the Red Lake mine trend: example from the Cochenour-Willans mine area, Red Lake, Ontario, with new key information from the Red Lake mine and potential analogy with the Timmins camp; Geological Survey of Canada, Current Research 2003-C21, 15 p.

Dubé, B., Williamson, K., McNicoll, V., Malo, M., Skulski, T., Twomey, T., and Sanborn-Barrie, M.
2004: Timing of gold mineralization at Red Lake, northwestern Ontario, Canada: new constraints from U-Pb geochronology at the Goldcorp High-grade Zone, Red Lake mine, and at the Madsen mine; Economic Geology, v. 99, p. 1611–1641.

Gosselin, P., and Dubé, B.
2005: Gold deposits of Canada: distribution, geological parameters and gold content; Geological Survey of Canada, Open File 4896, 105 p.

Grant, J.A.
1986: The isocon diagram — a simple solution to Gresens' equation for metasomatic alteration; Economic Geology, v. 81, p. 1976–1982.

Huston, D.L.
1993: The effect of alteration and metamorphism on wall rocks to the Balcooma and Dry River South volcanic-hosted massive sulphide deposits, Queensland, Australia; Journal of Geochemical Exploration, v. 48, p. 277–307.

MacGeehan, P. and Hodgson, C.J.
1982: Environments of gold mineralization in the Campbell Red Lake and Dickenson mines, Red Lake district, Ontario; *in* Geology of Canadian gold deposits, (ed.) R. W. Hodder; Canadian Institute of Mining and Metallurgy, Special Volume 24, p. 184–207.

Parker, J.R.
2000: Gold mineralization and wall rock alteration in the Red Lake greenstone belt: a regional perspective; Summary of Field Work and Other Activities, Ontario Geological Survey, Open File Report 6032, p. 22-1 – 22-28.
2002: Lithogeochemical data from the Red Lake Greenstone Belt, Northwestern Ontario; Ontario Geological Survey, Miscellaneous Release-Data, MRD113.

Penczak, R.S.
1996: The geological context of alteration and gold mineralization at the Campbell mine, Red Lake district, Ontario; M.Sc. thesis, Queen's University, Kingston, Ontario, 334 p.

Penczak, R.S. and Mason, R.
1997: Metamorphosed Archean epithermal Au-As-Sb-Zn-(Hg) vein mineralization at the Campbell mine, northwestern Ontario; Economic Geology, v. 92, p. 696–719.
1999: Characteristics and origin of Archean premetamorphic hydrothermal alteration at the Campbell gold mine, northwestern Ontario, Canada; Economic Geology, v. 94, p. 507–528.

Rogers, J.A.
1992: The Arthur W. White mine, Red Lake area, Ontario: detailed structural interpretation the key to successful grade control and exploration; Canadian Mining and Metallurgical Bulletin, v. 85, p. 37–44.

Sanborn-Barrie, M., Skulski, T., and Parker, J.R.
2001: Three hundred million years of tectonic history recorded by the Red Lake greenstone belt, Ontario; Geological Survey of Canada, Current Research 2001-C19, 30 p.
2004: Geology, Red Lake greenstone belt, western Superior Province, Ontario; Geological Survey of Canada, Open File 4594, scale 1:50 000.

Tarnocai, C.A.
2000: Gold mineralization at the Campbell mine, Red Lake greenstone belt, Uchi subprovince, Ontario; Ph.D. thesis, University of Ottawa, Ottawa, Ontario, 240 p.

Thompson, P.H.
2003: Toward a new metamorphic framework for gold exploration in the Red Lake greenstone belt; Ontario Geological Survey, Open File Report 6122, 52 p.

Tomlinson, K.Y., Stevenson, R.K., Hughes, D.J., Hall, R.P., Thurston, P.C., and Henry, P.
1998: The Red Lake greenstone belt, Superior Province: evidence of plume-related magmatism at 3 Ga and evidence of an older enriched source; Precambrian Research, v. 89, p. 59–76.

Twomey, T. and McGibbon, S.
2001: The geological setting and estimation of gold grade of the High-grade Zone, Red Lake Mine, Goldcorp Inc.; Exploration and Mining Geology, v. 10, p. 19–34.

Zhang, G., Hattori, K., and Cruden, A.
1997: Structural evolution of auriferous deformation zones at the Campbell Mine, Red Lake greenstone belt, Superior province; Precambrian Research, v. 84, p. 83–103.

Geological Survey of Canada Project GK4760-X15